Received: 29 May 2020 | Revised: 18 December 2020 | Accepted: 19 December 2020

DOI: 10.1111/ejn.15095

SPECIAL ISSUE ARTICLE

EJN European Journal of Neuroscience FENS WILEY

Eye movement-related brain potentials during assisted navigation in real-world environments

Anna Wunderlich[1] | **Klaus Gramann**[1,2,3]

[1]Technische Universität Berlin, FG Biopsychologie und Neuroergonomie, Berlin, Germany

[2]School of Computer Science, University of Technology Sydney, Sydney, NSW, Australia

[3]Center for Advanced Neurological Engineering, University of California, San Diego, CA, USA

Correspondence
Anna Wunderlich, Technische Universität Berlin, Sekr. KWT-1, Fasanenstr. 1 Eingang 1, 10623 Berlin, Germany.
Email: anna.wunderlich@tu-berlin.de

Funding information
Stiftung der deutschen Wirtschaft

Abstract

Conducting neuroscience research in the real-world remains challenging because of movement- and environment-related artifacts as well as missing control over stimulus presentation. The present study overcame these restrictions by mobile electroencephalography (EEG) and data-driven analysis approaches during a real-world navigation task. During assisted navigation through an unfamiliar city environment, participants received either standard or landmark-based auditory navigation instructions. EEG data were recorded continuously during navigation. Saccade- and blink-events as well as gait-related EEG activity were extracted from sensor level data. Brain activity associated with the navigation task was identified by subsequent source-based cleaning of non-brain activity and unfolding of overlapping event-related potentials. When navigators received landmark-based instructions compared to those receiving standard navigation instructions, the blink-related brain potentials during navigation revealed higher amplitudes at fronto-central leads in a time window starting at 300 ms after blinks, which was accompanied by improved spatial knowledge acquisition tested in follow-up spatial tasks. Replicating improved spatial knowledge acquisition from previous experiments, the present study revealed eye movement-related brain potentials to point to the involvement of higher cognitive processes and increased processing of incoming information during periods of landmark-based instructions. The study revealed neuronal correlates underlying visuospatial information processing during assisted navigation in the real-world providing a new analysis approach for neuroscientific research in freely moving participants in uncontrollable real-world environments.

KEYWORDS

blink-related potentials, gait artifacts, landmark-based navigation instructions, mobile EEG, spatial knowledge acquisition

Abbreviations: ANOVA, analysis of variance; bERP, blink event-related potential; EEG, electroencephalography; EOG, electrooculography; ERP, event-related potential; fERP, fixation event-related potential; GPS, Global Positioning System; IC, independent component; ICA, independent component analysis; LNC, late negative component; LPC, late positive component; sERP, saccade event-related potential.

Edited by: Pierfilippo De Sanctis

1 | INTRODUCTION

1.1 | Navigation assistance systems and spatial knowledge acquisition

Navigating and orienting in our environment are fundamental aspects of every-day activities. Common navigation tasks vary with regards to the distance traveled and familiarity with the environment. Accordingly, navigation tasks range from commuting to work, or grocery shopping to touristic trips, or long hikes to explore new areas. Increasingly, technology, i.e., navigation assistance systems, facilitates or even take over parts of these spatial orienting tasks. The frequent use of navigation aids, however, was shown to be associated with decreased processing of the environment (Ishikawa et al., 2008; Münzer et al., 2006) and to be adverse to the ability to successfully use spatial strategies when no navigation aid is available (Dahmani & Bohbot, 2020).

In previous studies, we demonstrated that the use of commercial navigation instructions that highlight an "intersection" (e.g., "Turn left at the next intersection!") leads to a decrease of landmark knowledge. This was especially detrimental regarding knowledge of landmarks at decision points with route direction changes (Gramann et al., 2017; Wunderlich & Gramann, 2018, 2020). These studies further demonstrated the successful incidental acquisition of landmark and route knowledge when landmark-based rather than standard instructions were used. The experimental setups in these studies ranged from simulated driving through a virtual world (Wunderlich & Gramann, 2018) to interactive videos of walking or actually walking through the real-world (Wunderlich & Gramann, 2020). The results revealed higher amplitudes of the event-related late positive component (LPC) at parietal leads with the cued recall of landmark pictures. The increased LPC was interpreted as reflecting the recollection of more spatial information which corresponded to better cued recall performance observed for landmark-based navigation instructions (Wunderlich & Gramann, 2018). Even though these studies provided new insights into spatial knowledge acquisition when assistance systems were used for navigation, they all addressed spatial knowledge acquisition *after* the assisted navigation phase providing no further insights into incidental spatial knowledge acquisition *during* navigation.

1.2 | Investigating brain activity during navigation in real-world studies

Overcoming the restrictions of established brain imaging methods (Gramann et al., 2011; Makeig et al., 2009), new mobile brain imaging devices allow for recording human brain activity *during* active navigation and in the real-world providing high ecological validity (Park et al., 2018). Real-world navigation includes natural interaction with a complex, dynamically changing environment and other social agents, as well as realistic visuals and soundscapes. However, mobile EEG recordings come with several problems. First, active movement through the real-world is associated with increasing noise in the recordings (Gramann et al., 2014). The EEG records data on the surface of the scalp that is the result of volume conducted brain and non-brain sources. The latter include biological sources (e.g., eye movement and muscle activity) as well as mechanical and electrical artifacts (e.g., loose electrodes, cable sway, electrical sources in the environment). A second problem lies in a multitude of external and internal events that are impossible to control but are naturally present when the real-world is used as an experimental environment to investigate cognitive phenomena. Some of these events might provoke artifactual activity with respect to the phenomena of interest (e.g., a startle response to a car horn or suddenly appearing pedestrians). Finally, tests in the real-world do not allow for the control of the number and timing of the events of interest that are usually presented in high numbers for the analysis of event-related brain activity (Luck et al., 2000).

The problem of inherently noisy data can be addressed by blind source separation methods such as independent component analyses (ICA, Bell & Sejnowski, 1995; Makeig et al., 1996). Removing non-brain sources from the decomposition allows for back-projecting only brain activity to the sensor level, using ICA as an extended artifact removal tool (Jung et al., 2000). The second problem, the multitude of random events, might be overcome by an averaging approach of event-related potentials (ERPs) to average out EEG activity that was not related to the processes of interest. However, to do so, the third problem has to be solved and a sufficiently high number of meaningful events has to be found for event-related analyses and the related activity extracted and separated from other or overlapping activity (Ehinger & Dimigen, 2019).

1.3 | Eye movement-related events and potentials

Physiological non-brain activity captured in the mobile EEG can be used as a source of meaningful events for the analyses of ERPs. Using such activity is non-intrusive to the ongoing task (Bentivoglio et al., 1997). and naturally occurring physiological events like eye blinks and saccades allow to parse the EEG signal into meaningful segments as they covary with visual information intake (Berg & Davies, 1988; Kamienkowski et al., 2012; Stern et al., 1984). Saccades suppress visual information intake starting 50 ms preceding a saccade-onset as well as during the saccade. Thus, each fixation following a saccade represents the onset of visual information intake. Event-related potentials using saccades can be related to either saccade onset, peak velocity, or saccade offset, with the latter being equivalent to the fixation-related potentials (fERP). Saccade-related brain potentials (sERP)

were used in many previous studies (Gaarder et al., 1964; Rämä & Baccino, 2010), especially in research investigating reading and text processing (Baccino, 2012; Dimigen et al., 2011; Marton & Szirtes, 1988) or visual search (Kamienkowski et al., 2018; Kaunitz et al., 2014; Ossandón et al., 2010).

The sERP starts with the parietal presaccadic spike potential, which represents the execution of the saccade as well as its attentional/motivational value (Sailer et al., 2016). The posterior positive component 80 ms from the saccade offset is labeled lambda response (Kazai & Yagi, 2003) which was shown to be sensitive to properties of the visual stimulus like luminance or contrast (Dimigen et al., 2011; Gaarder et al., 1964; Kaunitz et al., 2014; Kazai & Yagi, 2003). The sensitivity of the lambda response to the properties of incoming visual information as well as its close cortical origin renders the lambda response comparable to the P1 in stimulus-evoked ERPs (Kazai & Yagi, 2003). Thus, the P1 and lambda response seem to be elicited by the same perceptual process (Kaunitz et al., 2014). The subsequent P2 of the sERP at posterior leads was shown to be sensitive to the processing of context information (Marton & Szirtes, 1988) and semantic meaning of text information (Simola et al., 2009). Simola et al. (2009) showed a right hemispheric dominance of the P2 component when processing words versus non-words. In visual search, the parietal P2 demonstrated decreased amplitudes when fixating targets compared to distractors (Kamienkowski, Navajas, et al., 2012). In a later time window starting at 380 ms Kamienkowski et al. (2012) showed a positive component for targets only at frontal leads.

In contrast to saccades, blinks produce a longer interruption of the visual input stream (for a review see Stern et al., 1984). Despite startle, invasive external events or dry eyes, there are at least three different factors determining the timing of blink generation. First, in order to keep the efficiency of the visual input channel high, and to reduce interruptions in the visual information stream, blinks are combined with other eye movements (Evinger et al., 1994). Second, blinks likely occur after a period of blink suppression (e.g., during attention allocation) or when the processing mode changes. Thus, they can mark the end of an information processing chain (Stern et al., 1984). Third, in very structured tasks using for example stimulus-response pairs, blinks show a temporal relationship to stimulus presentation (Stern et al., 1984). Like saccades and fixations, blinks have been used for extracting event-related potentials (bERP). The bERP was shown to be sensitive to the parameters of the experimental environment or characteristics of the current task (Berg & Davies, 1988; Wascher et al., 2014). The long preceding pause of incoming visual information might make bERPs more similar to ERPs. In addition, the increased likelihood for blinks at the end of information processing steps qualifies the bERPs during natural viewing as a valuable source of insight about visual information processing and underlying cognitive processes.

Berg and Davies (1988) stated that the time point zero in bERPs comparable to ERP research is when the eyelid uncovers the pupils. This happens about 100 ms after the blink maximum and thus qualifies the occipital P200 and N250 referenced to the blink maximum as candidates to represent comparable processes like the P1/N1 complex of the stimulus-evoked potential. Based on the interpretation of the visual evoked activity in traditional ERP studies, the P200 in the bERP (P1 in ERP studies) would reflect an exogenous component related to the sensory processing of attended incoming visual information which is influenced by stimulus parameters like contrast. The N250 in the bERP (N1 in ERP studies) would be related to the allocation of attention to task-relevant stimuli and discrimination of stimulus features (Luck, 2005; Luck et al., 1990). A fronto-central P100 of the bERP was shown to be less pronounced and the following N200 to be more pronounced in a cognitive task when compared to a physical task or rest (Wascher et al., 2014).

Regarding later evoked components of the bERP, Berg and Davies (1988) described the posterior P300 to be more pronounced when subjects blinked under light as compared to blinking in darkness. In the latter case, the bERP P300 was nearly absent, implying that this P300 reflects the processing of incoming visual information. Accordingly, Wascher et al. (2014) found the posterior P300 to be most pronounced during rest, followed by the cognitive task and least pronounced during the physical task reflecting amplitude modulation due to information processing. The waveform of the component reminds of the P300 at posterior leads in traditional ERP studies and seems to be composed of several sub-components underlying different cognitive processes.

1.4 | Research goal and hypotheses

In this paper, we describe a means to deal with the previously specified issues arising from collecting mobile EEG during an ongoing task in the real-world. We show how both blink- and saccade-related potentials alongside gait-related activity in uncontrolled real-world environments can be extracted from IC source time series. These events can subsequently be analyzed to gain deeper insights into the ongoing brain activity accompanying information processing in the real-world.

In the present study, we used this approach to investigate human brain activity during assisted pedestrian navigation using standard or landmark-based auditory turn-by-turn instructions. We investigated how navigation instructions might change visual information processing and incidental spatial knowledge acquisition. We recorded and analyzed brain activity in the real-world, while participants navigated through the city of Berlin and were subsequently tested on their acquired spatial knowledge. Based on previously observed increased LPCs for landmarks presented in a cued-recall

task after navigation with landmark-based instructions, we expected landmark-based navigation instructions to generally shift attention toward information in the environment relevant for navigation. The accompanying improved spatial knowledge acquisition was assumed to lead to a better performance in the follow-up spatial tasks.

To investigate how navigators process the environment during assisted navigation, we used blink- and saccade-related potentials. These were extracted during the entire navigation task and analyzed separately for navigation periods at intersections where auditory navigation instructions were provided and periods were navigators walked straight segments of the route without navigation instructions. Eye movement-related potentials were expected to reveal differences between navigation instruction conditions, especially at intersections. Group differences during straight segments would indicate a general change in visual information processing. While this was an explorative study investigating eye movement-related brain potentials in a real-world navigation task, previous ERP studies and studies using eye movement-related brain activity in established laboratory settings allowed for some hypotheses about differences in evoked potentials. Based on earlier laboratory studies, we expected group differences in early visual components at posterior leads reflecting instruction-dependent visuo-attentional processes. Furthermore, we expected more pronounced later components over parietal leads representing information integration and memory encoding, while late potential differences over fronto-central leads were expected to reflect a different involvement of higher cognitive processes.

2 | MATERIALS AND METHODS

2.1 | Participants

The data of 22 participants (11 women) were analyzed with eleven participants in each navigation instruction condition. Their age ranged from 20 to 39 years ($M = 27.4$, $SD = 4.63$ years). Participants were recruited through an existing database or personal contact and received either 10 Euro per hour or course credit. All had normal or corrected to normal vision and gave informed consent prior to the study which was approved by the local research ethics committee of the Institute for Psychology and Ergonomics at the Technische Universität (TU) Berlin. Before the main experiment, participants filled out an online questionnaire to determine if they were familiar with the area where the navigation task would take place (Wunderlich & Gramann, 2020). After navigating the route, participants were again asked whether they had been familiar with the navigated route. In case participants stated familiarity with more than 50% of the route, they were excluded from the second part of the experiment and data analysis. In the final sample of 22 participants, familiarity ratings ranged from 0% to 40% ($M = 9.52\%$, $SD = 12.2\%$).

2.2 | Study design and procedure

The experiment consisted of two parts and lasted approximately 3 hr in total. In the first part, participants walked a predefined route through the district of Charlottenburg, Berlin in Germany, using an auditory navigation assistance system. In the second part, directly after the navigation task, participants were transported back to the Berlin Mobile Brain/Body Imaging Lab (BeMoBIL) at TU Berlin to run different spatial tests. Participants had not been informed about the spatial tasks and that they would be tested on the environment after the navigation task.

During the navigation task, participants followed the auditory navigation instructions to navigate along a 3.2 km long, predefined, unfamiliar route with twenty intersections. There were two groups of participants, either receiving standard or landmark-based navigation instructions prior to each intersection. Based on previous results (Gramann et al., 2017; Wunderlich & Gramann, 2018, 2020), landmark-based instructions referenced a landmark at each intersection and provided more detailed information about this landmark. One example of navigation instruction for this landmark-based condition was "Turn left at the UdK. The UdK is the biggest University of Arts in Europe." This contrasted with the standard navigation instruction condition that used instructions like "Turn left at the next intersection." Previous to the navigation task, it was pointed out to the participants that they should follow the auditory turn-by-turn instructions and be aware of other traffic participants, especially while crossing streets. Furthermore, in case they feel lost, they were asked to stop and turn to the experimenter who was shadowing the participant with two to three meters distance. The presence of the experimenter ensured the participant's safety as well as the correct course of the route. The experimenter manually triggered the auditory navigation instructions using a browser-based application on a mobile phone. Participants received the auditory navigation instructions by Bluetooth in-Ear headphones at predefined trigger points in the environment. After walking for approximately 40 min, the participants arrived at the end of the route. There, they were instructed to rate their subjective task load during navigation using the National Aeronautics and Space Administration Task Load Index (NASA-TLX; Hart, 2006; Hart & Staveland, 1988). Additionally, they filled in three short questions regarding their prior knowledge of the route.

The second part of the experiment took place at the BeMoBIL. There, the first task was to draw a map of the route on an empty sheet of paper (DIN A3) and secondly to

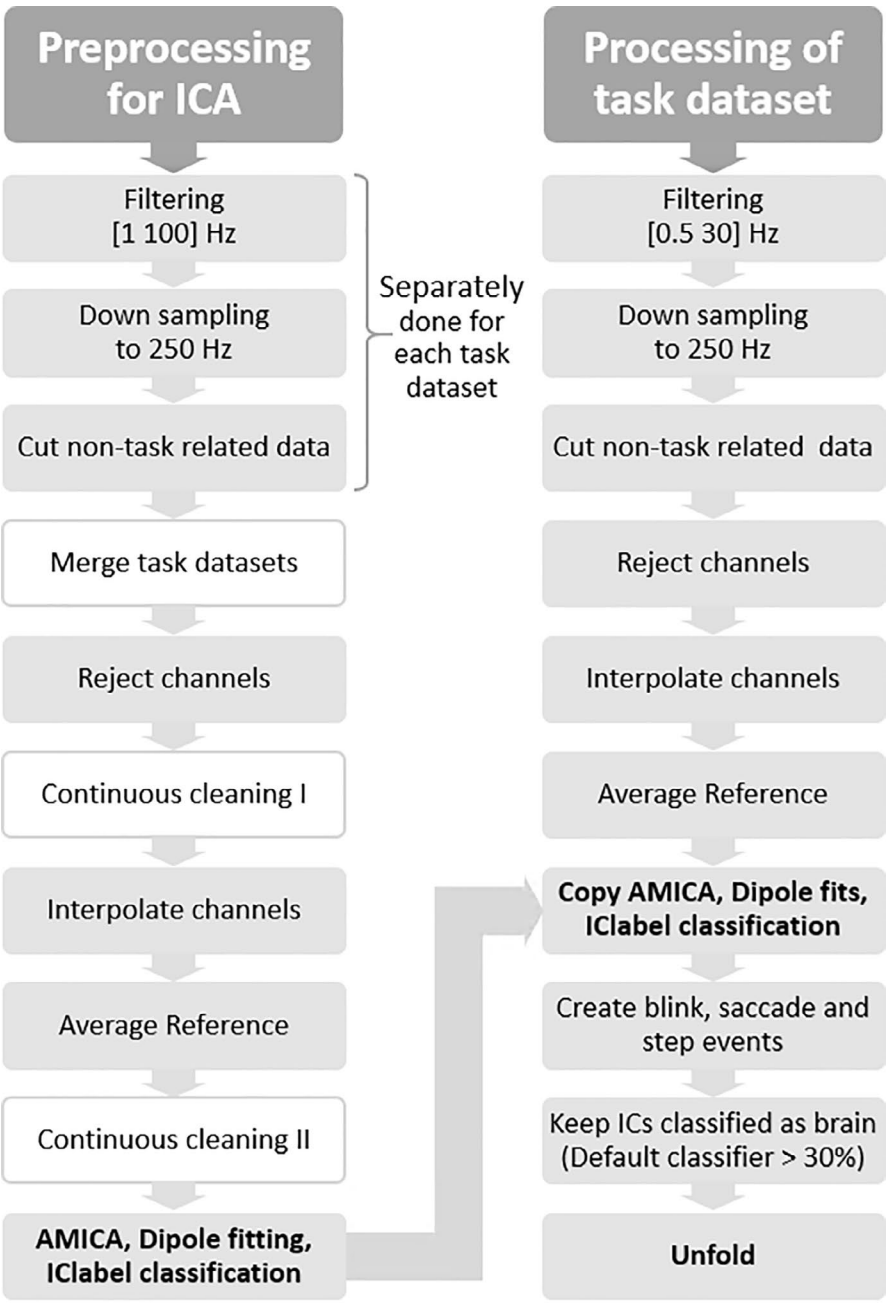

FIGURE 1 EEG data processing from raw data to ICA computation (left) and from raw task data to the use of the unfold toolbox (right). Additional analysis steps in the ICA preprocessing have white boxes to emphasize the otherwise parallel processing

solve a cued-recall task. In the latter task, sixty landmark pictures were given as cues and the required response included the respective route direction. The randomly shown landmarks had been either located at intersections (and mentioned in the landmark-based navigation instructions) or at straight segments of the route (without navigation instructions), or they were similar in appearance but not part of the previously navigated route. In the end, demographic data as well as individual navigation habits, and subjective spatial ability ratings using the Santa Barbara Sense of Direction Scale (SBSOD; Hegarty et al., 2002) and the German questionnaire Fragebogen Räumliche Strategien (FRS; Münzer et al., 2016; Münzer & Hölscher, 2011) as well as perspective taking (PTSOT; Hegarty & Waller, 2004) were collected.

2.3 | Electroencephalography

2.3.1 | EEG data collection

The EEG was recorded continuously during the navigation task and the subsequent laboratory tests using an elastic cap with 65 electrodes (eego, ANT Neuro, Enschede, The Netherlands). Electrodes were placed according to the extended 10% system (Oostenveld & Praamstra, 2001). All electrodes were referenced to CPz and the data were collected with a sampling rate of 500 Hz. One electrode below the left eye was used to record vertical eye movements. Time synchronization and disk recording of the EEG data stream and the event marker stream from the mobile application and

task paradigm was performed using Lab Streaming Layer (LSL, https://github.com/sccn/labstreaminglayer; Accessed on November 1, 2020).

2.3.2 | EEG data processing

For EEG data processing, the MATLAB toolbox EEGLAB was used (Delorme & Makeig, 2004). The raw EEG data of both the navigation phase and the cued-recall task were high pass filtered at 1 Hz, low pass filtered at 100 Hz using the EEGLAB filter function *eegfilter()*, and subsequently resampled to 250 Hz (see Figure 1, left column). The pre- and post-task phases of the EEG data were removed. Afterward, the two separate datasets of each participant were merged into one dataset and channels that were subjectively judged as very noisy, flat, or drifting were manually rejected ($M = 3.79$, $SD = 1.77$, $Min = 1$, $Max = 8$). Continuous data cleaning was applied twice using the *pop_rejcont()* function for frequency limits from 1 to 100 Hz and default settings for all other parameters.[1] Rejected channels were interpolated using a spherical spline function and the data were re-referenced to the average reference. Time-domain cleaning before interpolation and re-referencing targeted artifacts on a single channel level prohibiting the inflation of single noisy channels when re-referencing to average reference. A second-time-domain cleaning was applied to remove the remaining artifactual data.

Subsequently, the data were submitted to independent component analysis (ICA, Makeig et al., 1996) using the Adaptive Mixture ICA (AMICA, Palmer et al., 2011). The resultant independent components (ICs) were localized to the source space using an equivalent dipole model as implemented in the dipfit routines (Oostenveld & Oostendorp, 2002). Finally, the resultant ICs were classified as being brain, muscle or other processes using the default classifier of IClabel (Pion-Tonachini et al., 2019).

The original sensor data were preprocessed using identical processing steps as described above save different filter frequencies and no time-domain data cleaning (see Figure 1, right column). The respective weights and sphere matrices from the AMICA solution were applied to the preprocessed navigation dataset. In addition, the equivalent dipole models and IClabel classifications for each participant and IC were transferred to the respective task dataset allowing for the extraction of events based on the complete duration of the task.

[1]Parameters used for the EEGLAB function pop_rejcont: cleaning based on all electrodes; epoch length of 0.5 s; epoch overlap of 0.25 s; frequency limits to consider for thresholding [10 50]; frequency upper threshold 10 dB; four contiguous epochs necessary to label a region as artifactual; once a region of contiguous epochs has been labeled as an artifact, additional trailing neighboring regions of 0.25 s on each side were added; selected regions were removed from the data; spectrum was computed within the function; hamming was used as taper before fast Fourier transformation (FFT).

2.4 | Event extraction from IC time course

The event extraction is summarized in Figure 2. Blinks were identified using one IC from the individual decompositions that reflected vertical eye movements as described in Lins et al. (Lins et al., 1993). In case of more than one candidate for the vertical eye IC, the component showing a better signal to noise ratio for blink deflections and/or less horizontal eye movement was chosen based on subjective inspection.

For detecting blinks, the associated component activation time course was filtered using a moving median approach (window size of twenty sample points equaling 80 ms). Moving median approaches smooth without changing the steepness of the slopes in the data (Bulling et al., 2010). To allow for automated blink peak detection, all individual IC time courses were standardized to a positive peak polarity. Peak detection was performed using the MATLAB function *findpeaks()* applied to the filtered IC activation. Parameters used were a *minimal peak distance* of 25 sample points (100 ms) to avoid directly following blinks to be selected. Further, peaks were restricted to a *minimal peak width* of 5 (20 ms) and *maximal peak width* of 80 sample points (320 ms) to suppress potential high-amplitude artifacts or slow oscillations from being counted as a blink. The following two parameters were automatically defined for each dataset individually to take care of interindividual differences in the shape of the electrical signal representing a blink: the 90-percentile of the filtered activation data was applied to define a threshold of *minimal peak prominence*. This parameter ensured the successful separation of detected peaks from the background IC activity. For the absolute *minimal peak height*, a threshold was defined using the 85-percentile of the filtered activation data. For each peak location, an event marker with the name *blink* was created in the EEG dataset at the time point of maximum blink deflection.

Saccades were identified using two ICs from the individual decompositions that reflected vertical and horizontal eye movements, respectively (according to Lins et al., 1993). Vertical eye movement ICs were the same as used for blink detection. For the horizontal eye movement ICs, the IC with the most characteristic scalp map and rectangular activity in the activation time course reflecting horizontal eye movements was chosen based on subjective inspection. The associated component activation time courses were filtered using a moving median approach (window size of 20 sample points equaling 80 ms). The electrooculogram (EOG) activity was calculated using the root mean square of the smoothed time courses (Jia & Tyler, 2019). For saccade maximum velocity detection, the first derivative was taken and squared to

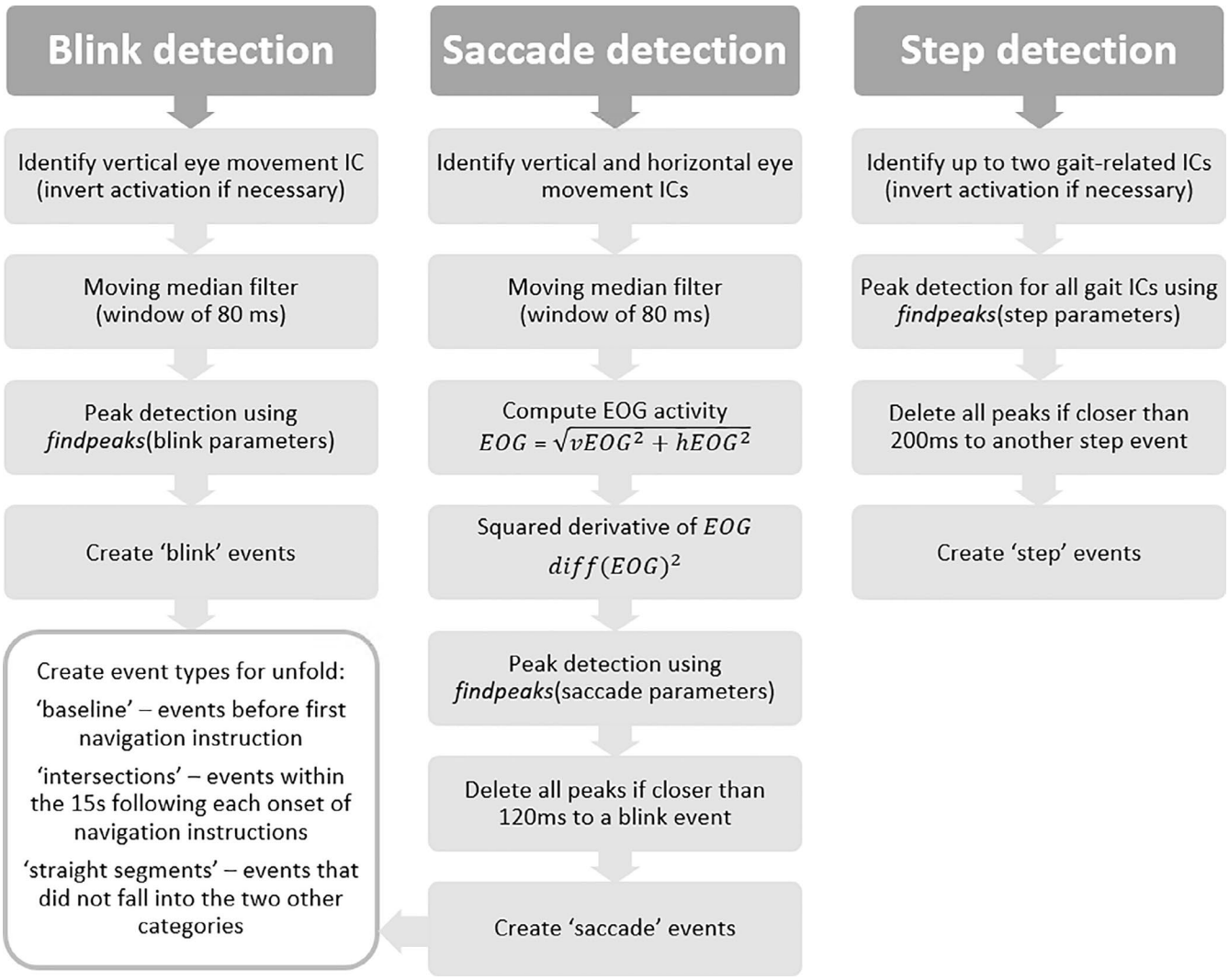

FIGURE 2 Analysis steps for the extraction of events from the respective IC activation(s): blink (left), saccade (middle), and step events (right). The respective parameters for the findpeaks() functions can be found in the text

increase the signal-to-noise-ratio. The function *findpeaks()* was applied to the squared derivative of the EOG activation. Parameters used were a *minimal peak distance* of 25 sample points (100 ms). Peaks were restricted to a *minimal peak width* of 1 (4 ms) and *maximal peak width* of 10 sample points (40 ms). The 90-percentile of the squared derivative of the EOG was applied for *minimal peak prominence* as well as for the *minimal peak height* threshold. In case identified peaks were closer than 30 sample points (120 ms) to a blink event, these peaks were not taken for saccade event extraction to avoid taking saccades into account that appeared during eyes closed periods. For each of the remaining peaks, an event marker called *saccade* was created in the EEG dataset at the time point of maximum saccade velocity (middle of the saccade).

Gait-related EEG activity was identified based on IC activation time course, scalp maps, and spectra from each individual decompositions. Up to two ICs were chosen manually that reflected gait cycle-related activity as described previously in studies comparing measures of kinematics and EEG activity (Jacobsen et al., 2020; Kline et al., 2015; Knaepen et al., 2015; Oliveira et al., 2017; Snyder et al., 2015). No filtering or smoothing was applied to the associated component activation time courses that showed a pronounced waveform at approximately 2 Hz. Inverting of time courses for some ICs was performed to align peak amplitudes on top of the slow-wave maxima. To extract single steps of the gait cycle, *findpeaks()* was applied to both IC activations consecutively. Peaks were restricted to a *minimal peak width* of 5 (20 ms) to take advantage of the high-frequency part and *maximal peak width* of 150 sample points (600 ms) to detect the slow-wave peaks. *Minimal peak distance* was set to 100 sample points (400 ms) to avoid that the high-frequency part and the slow-wave peak were both used for event extraction. The 80-percentile of the IC activation time course was applied for *minimal peak prominence* and as a threshold for *minimal peak height*. In case of step events identified in the two ICs being closer than 50 sample points (200 ms) one of the

respective events was not taken into account for event generation. For each remaining detected peak, an event marker named *step* was created in the EEG dataset.

Afterward, every dataset was visually checked to validate blink, saccade, and gait events according to previous reports (Kline et al., 2015; Lins et al., 1993). To enable the comparison of blink- and saccade-related brain activity in different phases of the navigation task, we included different labels according to the task phases. The first event type was labeled *baseline* in case the event appeared before the first navigation instruction and thus was unaffected by the navigation instruction conditions. This baseline phase lasted on average six minutes (M = 352s, SD = 200 s). A second event type was labeled *intersections* in case the event took place within the 15 s following the onset of each of the twenty navigation instructions (in sum 300 s). The event type *straight segments* were used for all other remaining events in the navigation phase. On average, the time interval between two navigation instructions was 123 s. The number of events in each category can be seen in Table 1.

2.5 | Source-based EEG data cleaning

Subsequently, all ICs with a classification probability lower than 30% in the category *brain* were removed from the dataset and the data were back-projected to the sensor level. This way the number of ICs per participant was reduced to M = 13.3 ICs (SD = 4.50 ICs, Min = 5 ICs, Max = 22 ICs). Considering the instruction conditions, this IC reduction did not lead to unbalanced numbers of ICs between the two instruction condition groups (standard: M = 13.1 ICs, SD = 5.12 ICs, Min = 5 ICs, Max = 22 ICs; landmark-based: M = 13.5 ICs, SD = 4.74 ICs, Min = 6 ICs, Max = 18 ICs).

2.6 | Unfolding of event-related activity

The last data processing step on the single-subject level was the application of the unfold toolbox to the continuous data (Ehinger & Dimigen, 2019). This toolbox allows for a regression-based separation of overlapping event-related brain activity. As the extracted eye and body movement events in the navigation task overlapped with each other (Dimigen et al., 2011) and/or were temporally synchronized for some participants, it is a valuable tool to consider and control for overlapping ERPs and individual differences.

Following the published analysis pipeline of (Ehinger & Dimigen, 2019), we defined a design matrix with blink, saccade, and step events and 64 channels. We included the categorical factor *navigation phase* (baseline, intersections, straight segments) for the blink and saccade events into the regression *formula: y = 1 + cat(navigation phase)*. For the step events, we only computed the intercept: *y = 1*. After applying the continuous artifact detection of the unfold pipeline and exclusion set to *amplitude threshold* of 80 μV, we time-expanded the design matrix according to the *timelimits* of −500 ms and 1,000 ms referring to the event timestamp. Afterward, we fitted the general linear model and extracted the intercept and beta values considering −500 ms to −200 ms for baseline correction (similar to Wascher et al., 2014).

While the blink and saccade-related potentials were considered as informative for the analysis of visual information processing during navigation, the step events were only used to control for their individual impact on the blink and saccade-related potentials. The intercept and beta values of the general linear model built the basis for a comparison between participants. Unfolded event-related potentials for all event types were computed for all electrodes and used for statistical analysis of group differences. The ERPs of participants

TABLE 1 Number of blink, saccade, and step events for all participants and separated by navigation instruction condition and navigation phase

	Number blink events			Number saccade events			Step
	Baseline	Intersections	Straight segments	Baseline	Intersections	Straight segments	All
Standard instruction condition							
M	214	213	1,385	652	666	4,386	4,216
SD	142	81	592	224	113	1,104	1,033
Min	80	99	693	294	430	3,184	3,131
Max	572	355	2,730	996	857	6,808	6,878
Landmark based instruction condition							
M	183	193	1,236	559	794	4,307	3,994
SD	128	76	623	281	180	1,181	850
Min	68	89	384	184	366	1,893	1,762
Max	525	368	2,907	1,307	1,023	5,818	5,166

Abbreviations: M, mean; Max, Maximum; Min, Minimum; *SD*, standard deviation.

within one navigation instruction condition and navigation phase were averaged and plotted alongside with twice the standard error of the mean (*SEM*) for FCz and as scalp map for five concatenated time windows.

2.7 | Statistical analysis

We tested for group differences in individual and subjective measures using *t* tests of independent samples. The number of free-recalled landmarks in the sketch map and the sensitivity d′ of the cued-recall task were tested using each time a 2 × 2 mixed measure ANOVA with the between-subject factor navigation instruction condition (standard versus landmark-based) and the within-subject measure landmark location (intersections versus straight segments). The acquired route knowledge was compared between navigation instruction conditions for the landmarks at intersections using a *t* test of independent samples.

Statistical analysis on blink- and saccade-related brain potentials was performed for the interaction of navigation instruction condition (standard versus landmark-based) and baseline-corrected navigation phase (intersections versus straight segments). Group difference plots of the ERPs for both navigation phases were investigated to find time windows revealing significant differences between the navigation instruction conditions after the single-trial baseline ending at −200 ms. To define statistical significance between the unpaired values, the EEGLAB function *statcondfieldtrip()* was used. Due to this, a 10,000-fold permutation testing was applied followed by a cluster-based correction for family-wise error. If the returned probability corrected two-tailed *p*-value was below 0.05, the sample was marked as statistically significant.

3 | RESULTS

3.1 | Questionnaires

Using all questionnaire data, we checked for potential differences between the two experimental groups. When asking about the navigation assistance use, groups differed with respect to the use of navigation support (Item: "I use a navigation aid because I cannot find my way otherwise.") The control group demonstrated less use of navigation aids ($M = 2.73$, $SD = 2.05$) compared to the landmark-based navigation instruction group ($M = 4.45$, $SD = 2.11$; $t_{(20)} = -1.94$, $p = 0.066$, $d = 0.83$). No other items indicated differences between instruction groups (p's > 0.10). In addition, one item of the FRS targeting subjective orienting ability revealed a group difference. Navigators of the standard instruction group rated higher ($M = 4.64$, $SD = 1.43$) compared to the landmark-based navigation instruction group ($M = 3.00$, $SD = 1.67$; $t_{(20)} = 2.46$, $p = 0.023$, $d = 1.05$) in the item: "If I walk through an unfamiliar city, I know the direction of the start and goal location." All other items and the three factors of the FRS showed no significant differences (all p's > 0.171). The results of the SBSOD, the PTSOT, and the route familiarity after navigation showed no differences between the groups (all p's > 0.261).

Participants stated their task-related load after assisted navigation on six subscales of the NASA-TLX ranging from 1 to 100. The data revealed a difference of the two navigation instruction groups in the physical load assessment (standard: $M = 38.5$, $SD = 23.5$; landmark-based: $M = 20.6$, $SD = 15.9$; $t_{(20)} = 2.08$, $p = 0.050$, $d = 0.89$) and a trend regarding the subjective mental load (standard $M = 22.6$, $SD = 16.2$; landmark-based: $M = 37.5$, $SD = 18.4$; $t_{(20)} = -2.01$, $p = 0.058$, $d = 0.86$). All other subscales showed no difference between instruction groups (all *p's > 0.177*). There were no differences in walking speed between the instruction groups (standard $M = 4.76$ km/h, $SD = 0.35$ km/h; landmark-based: $M = 4.86$ km/h, $SD = 0.34$ km/h; $t_{(20)} = -0.68$, $p = 0.506$).

3.2 | Spatial knowledge acquisition

Free-recall of landmark knowledge was compared using a 2 × 2 ANOVA with the between-subject factor navigation instruction condition (standard versus landmark-based) and within-subject factor landmark type (intersections versus straight segments). The dependent variable analyzed was the number of correct landmarks marked in the sketch map. The main effect of navigation instruction condition ($F_{(1,20)} = 30.5$, $p < 0.001$, $\eta^2_p = 0.604$) as well as the main effect landmark type were significant ($F_{(1,20)} = 31.0$, $p < 0.001$, $\eta^2_p = 0.608$). The interaction effect also reached significance ($F_{(1,20)} = 25.9$, $p < 0.001$, $\eta^2_p = 0.564$). Post hoc contrasts of the interaction revealed that the number of correctly drawn landmarks at intersections was higher for the landmark-based navigation instruction condition ($M = 9.91$, $SE = 0.92$, $p < 0.001$) when compared to the standard navigation instruction condition ($M = 1.91$, $SE = 0.92$). The number of correctly drawn landmarks at straight segments was comparably low across navigation instruction conditions ($p = 0.721$).

The performance of the cued-recall task was used to compute the dependent variable d' representing the sensitivity of landmark recognition using signal detection theory. Its values were then tested in a 2 × 2 ANOVA with the between-subject factor navigation instruction condition (standard versus landmark-based) and within-subject factor landmark type (intersections versus straight segments). The main effect navigation instruction condition ($F_{(1,20)} = 3.53$, $p = 0.075$, $\eta^2_p = 0.150$) and the main effect landmark type

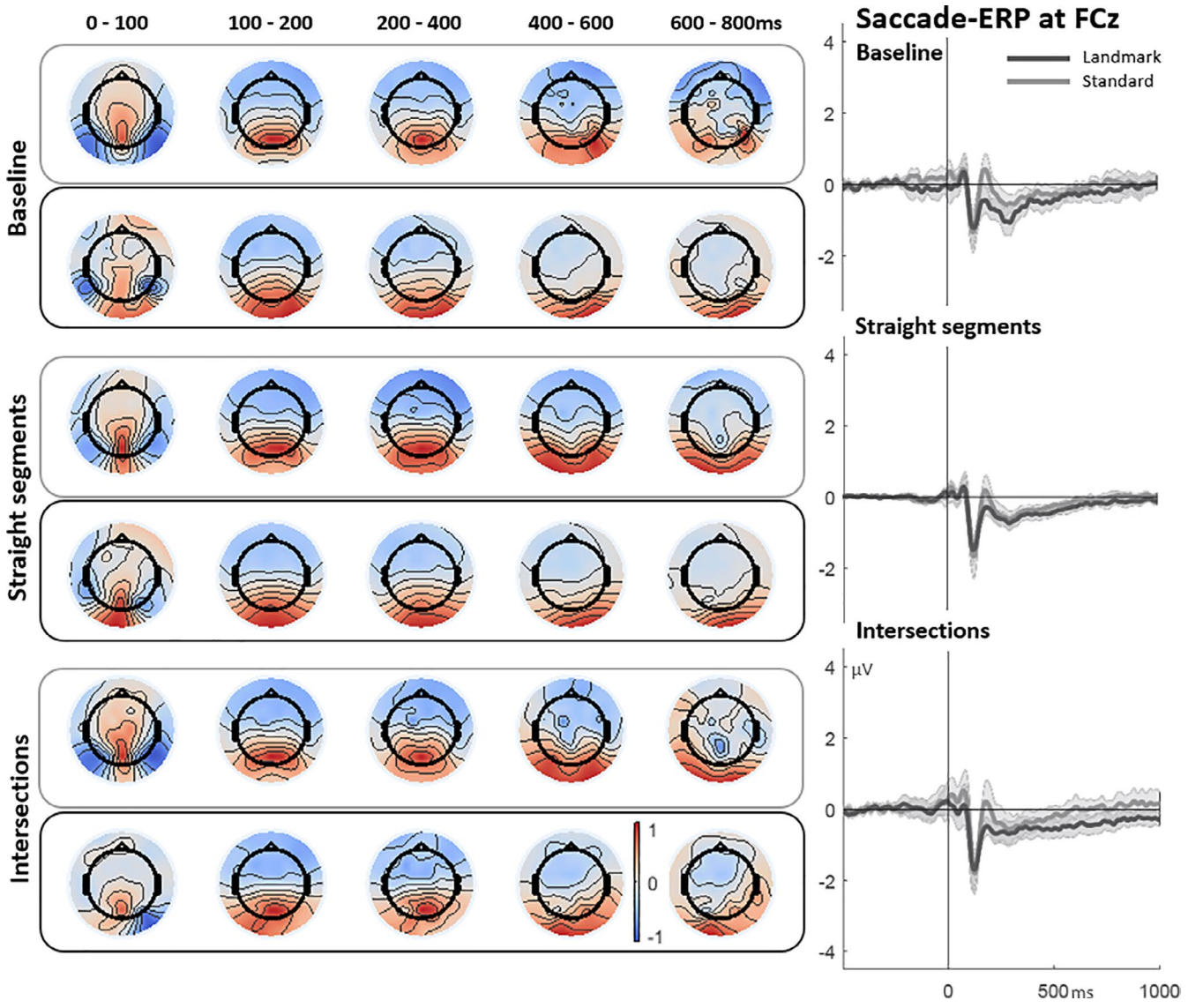

FIGURE 3 Saccade-related potentials. Left panel displays the topography of the activity averaged across time windows (100 ms duration for early and 200 ms duration for late components). Topography was plotted separately for each navigation instruction condition (light grey – standard, dark grey – landmark-based) and navigation phase (baseline, straight segments, intersections). Right panel shows the voltage over time plot of the respective saccade-related potential at FCz. The sERPs were baseline corrected by subtracting the average of -400 to -200 ms. Positivity is plotted upwards

showed a trend toward significance at the level of 0.05 ($F_{(1,20)} = 4.22$, $p = 0.053$, $\eta^2_p = 0.174$). The interaction of both factors reached significance ($F_{(1,20)} = 6.51$, $p = 0.019$, $\eta^2_p = 0.246$). Post hoc contrasts testing navigation instruction conditions showed that the recognition sensitivity for landmarks at intersections was higher for the landmark-based navigation instruction condition ($M = 2.47$, $SE = 0.25$, $p = 0.009$) compared to the standard navigation instruction condition ($M = 1.47$, $SE = 0.25$). The detection sensitivity for landmarks at straight segments was comparable across navigation instruction conditions ($p = 0.584$).

The incidentally acquired route knowledge as reflected in the percentage of correct route responses to landmarks at intersections was tested using an ANOVA with the between-subject factor navigation instruction condition (standard versus landmark-based). The significant main effect ($F_{(1,20)} = 11.2$, $p = 0.003$, $\eta^2_p = 0.358$) revealed that the landmark-based navigation group showed better performance ($M = 69.1\%$, $SE = 4.14\%$) than the control group ($M = 49.5\%$, $SE = 4.14\%$).

3.3 | Saccade-related potentials

The order and polarity of sERP components were comparable across navigation instruction conditions and navigation phases (see Figure 3). Amplitudes increased gradually from frontal to occipital leads as well as from lateral leads toward

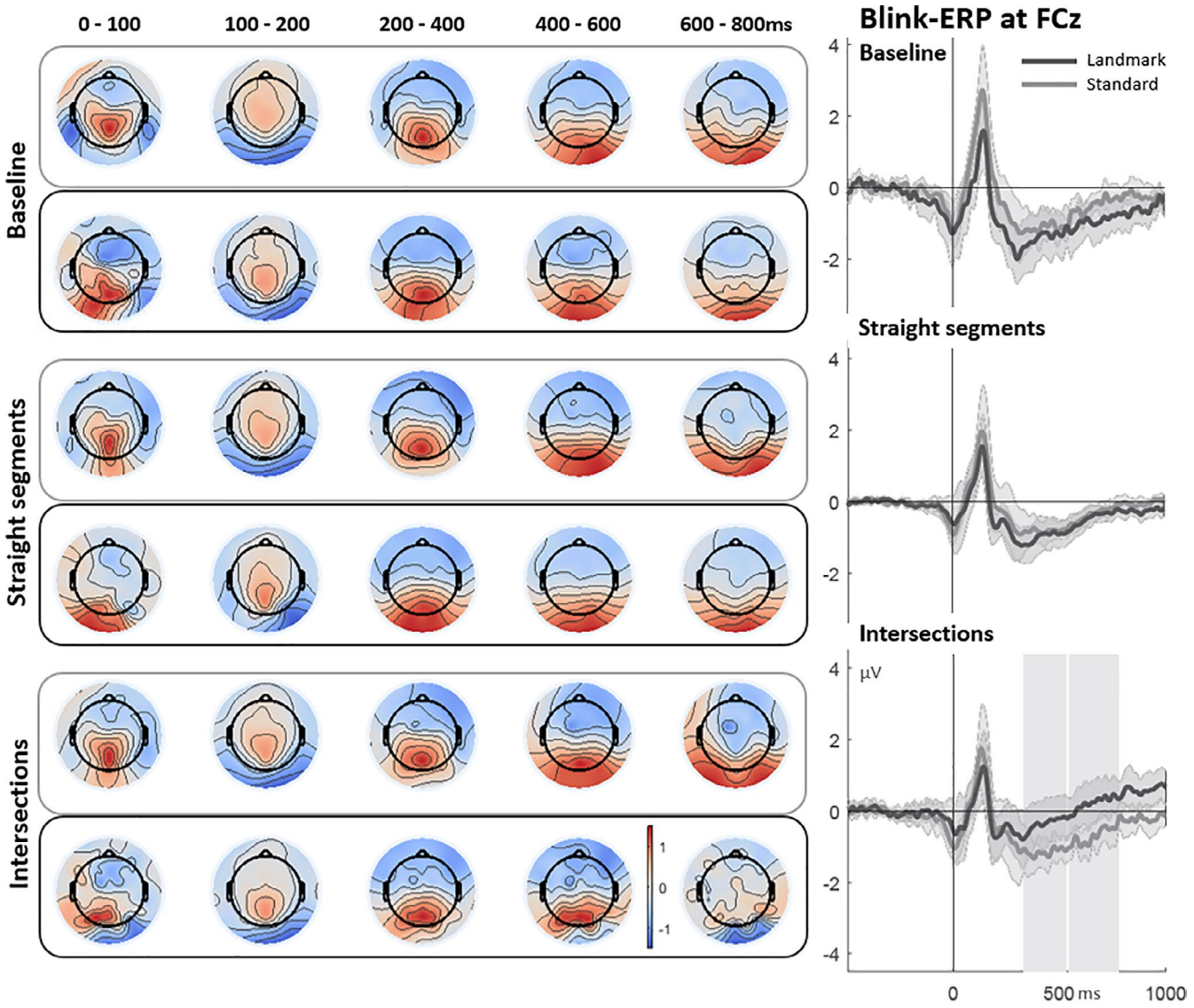

FIGURE 4 Blink-related potentials. Left panel displayes the topography of the activity averaged across time windows (100 ms duration for early and 200 ms duration for late components). Topography was plotted separately for each navigation instruction condition (light grey – standard, dark grey – landmark-based) and navigation phase (baseline, straight segments, intersections). Right panel shows the voltage over time plot of the respective blink-related potential at FCz. The bERPs were baseline corrected by subtracting the average of -400 to -200 ms. The grey rectangular areas represent time windows where samplewise significant differences between the navigation instruction conditions were found in the beta values of the respective navigation phase. Positivity is plotted upwards

the central midline. We labeled each peak using the polarity and the latency rounded to a multiple of 50 ms. In case, there were already established names to be found in sERP and fERP literature, we added the respective references when introducing these components.

The *presaccadic spike potential* or *P0* was observed at the majority of electrodes about 10–20 ms preceding the saccade event.

At frontal leads, a first negative component (*N100*) following the saccade event became visible at around 80 ms and peaked around 120 ms with an amplitude maximum of −2 µV at Fz. After the N100, a positive component was observed peaking around 160 ms. Subsequently, the potential slowly returned to the baseline without further dissociable components. The peak amplitude of the N100 decreased from frontal leads toward more central electrodes.

At parietal and occipital leads a pronounced *P100* or *lambda response* was elicited peaking at 110 ms. The P100 had the highest amplitude at POz with 6 µV. Following the P100, a negative component (*N150*) with a minimum at 160 ms became visible. After this N150, a second positive component (*P200*) evolved peaking around 200 ms at Pz and POz and around 300 ms at Oz. Afterward, the potential slowly returned to its baseline. The parietal P100 was slightly more pronounced over the right hemisphere when compared to left hemispheric leads.

3.4 | Blink-related potentials

The bERP revealed a different pattern of peaks compared to the sERP (see Figure 4). The order and polarity of components were the same across bERPs for different navigation instruction conditions and navigation phases. All components were more pronounced at the central midline as compared to right or left hemispheric electrodes.

From frontal to central sites, the bERP revealed a first negative component when the eyes were completely closed (*N0*). After this N0, the frontal bERP activity showed a first positive component (*P150*) reaching a maximum of about 2 μV around 140 ms after the blink at frontal leads with decreasing amplitudes toward lateralized leads. A second negative component was observed around 200 ms (*N200*) which was most pronounced at frontal leads. A second but relatively small positivity peaked around 50 ms later (*P250*), followed by a third negative component around 300 ms (*N300*). This N300 was less pronounced than the previous N200 and formed a plateau for about 200 ms before returning to the baseline with an additional very small component at about 500 ms. This late negative component will be referred to as the late negative component (*LNC*).

Parietal to occipital leads revealed a small elevation peaking at time point zero (*P0*) as a counterpart to the frontal N0. This was followed by negativity (*N100*) with increasing amplitudes and latencies from parietal to occipital sites (Pz: 0.8 μV, 110 ms; POz: −0.5 μV, 120 ms; Oz: −2.5 μV, 130 ms). The time shift between electrode sites of the latter component was also revealed in the following positive Peak (*P150*). The maximal amplitude was elicited at Pz with 4 μV and a latency of 160 ms. At Oz the latency of the remaining peak of the positivity was located around 200 ms post-event (*P200*) and reached 0 μV in the standard as compared to 2 μV in the landmark-based navigation instruction condition. This instruction dependent variation was visible in all navigation phases. After the P150, a second negative component (*N250*) peaked at about 1.5 μV with a latency of 230 ms at electrodes Pz and POz. At Oz, the negativity was temporally aligned with the one at Pz and POz and the peak-to-peak difference to the previous positivity constant for both experimental groups. Another positive component followed with a peak around 300 ms (*P300*) most pronounced at POz with about 3 μV. Reaching P300 the difference between the navigation instruction conditions at Oz leveled out. Finally, also at parietal to occipital leads a small component at approximately 600 ms was noticeable combined with an increased flattening of the slope compared to before.

3.5 | Differences between navigation instruction conditions

The results of the statistical analysis are displayed as grey bars in Figure 4. The ERPs were tested samplewise for significant differences between the navigation instruction conditions and

TABLE 2 Significant time windows in the blink- and saccade-related potentials

Event	Phase	Electrode position			Time in ms	Peak in ERP	Instruction condition with higher values
		Left	Center	Right	Start–end		
Blink	Intersections			F2	280–408	N300	Landmark-based
		FT7			368–476	N300	Standard
		FC1			552–772	LNC	Landmark-based
			FCz		336–532	N300	Landmark-based
			FCz		548–780	LNC	Landmark-based
		CP5			208–408	P300	Standard
		P5			188–376	P300	Qualified by BL diff
	Straight segments	FC3			656–804	LNC	Qualified by BL diff
		FC1			640–788	LNC	Landmark-based
		CP5			196–392	P300	Standard
		P7			200–312	P300	Qualified by BL diff
		P5			196–264	P300	Qualified by BL diff
		P3			196–324	P300	Qualified by BL diff
		P1			172–320	N250, P300	Standard
Saccade	Straight segments			F2	140–328	N300	Qualified by BL diff
		FC1			188–320	N300	Qualified by BL diff
		CP1			776–880	LNC	Qualified by BL diff

Abbreviations: BL diff, difference between the instruction conditions in the baseline phase; ERP, event-related potential; LNC, late negative component.

separately for events at straight segments and at intersections. To this end, the event-related activity of each participant was controlled for by the respective event-related activity before the first navigation instruction (baseline phase) using the beta values provided by the unfold toolbox.

Blink-related potentials differed in amplitude dependent on the navigation instruction conditions, irrespective of baseline differences, at F2, FT7, FC1, CP5, P5, and FCz for the intersections and at FC3, FC1, CP5, P7, P5, P3, and P1 for the straight segments. In the saccade-related potentials, significant differences were observed only for the straight segments at F2, FC1, and CP1.

The timing of the significant differences and their accompanying peaks in the event-related potentials are listed in Table 2. Additionally, the respective navigation instruction condition that showed higher absolute event-related amplitudes in this time window is listed in the last column. Saccade-related potentials differed between the two groups only during the baseline phase of the task.

4 | DISCUSSION

This study investigated the neural basis of visuospatial information processing of pedestrians navigating through a real city guided by an auditory navigation assistance system. The auditory navigation instructions were either standard navigation instructions providing turning instructions referring to the next intersection or landmark-based navigation instructions referring to a salient object at the upcoming intersection and providing explanatory information about this landmark object. The changes in visual information processing during assisted navigation in the real-world were investigated by extracting saccade- and blink-related potentials from the recorded mobile EEG data, while controlling for gait-related activity. This way a sufficient number of events for analyzing event-related brain activity in an otherwise uncontrolled real-world environment was attained. The resulting blink-based ERPs proved to be sensitive to the experimental manipulations of auditory navigation instructions. We discuss these results alongside with group differences in individual measures, spatial task performance, and the data processing pipeline.

4.1 | Subjective task load

The ratings of the NASA-RTLX showed that the task load during the assisted navigation was rather low and overall comparable across experimental groups. However, the individual ratings of the subscales physical and mental load did not support the assumption that the subjectively experienced load was comparable for both navigation instruction conditions. The trend toward higher mental load in the landmark-based instruction group contrasts with previous findings during simulated driving (Wunderlich & Gramann, 2018). Still, both group averages of pedestrian navigation were lower compared to the simulated driving experiment. A possible explanation is that walking is slower as well as more automated than simulated driving and in turn requires less effort. This lower effort in the primary locomotion task may have allowed participants to become more aware of the demands of the navigation task, especially since landmark-based instructions are novel and might have fostered attention to the navigation task. The group difference in the subjectively perceived physical load is more difficult to explain as all participants had the same route length and were instructed to walk at their preferred speed. Objective measures also support the comparable physical demand as walking speed did not differ between groups. This difference might be a complementary effect on the subjectively experienced mental load. Participants in the control group were not attending to familiar navigation instructions and might have concentrated on the physical aspects of the relatively long path perceiving the primary locomotion task more demanding.

4.2 | Spatial knowledge acquisition

Incidentally acquired landmark knowledge was tested in a free- and a cued-recall task. When sketching the navigated route on an empty sheet of paper, participants in the landmark-based instruction condition were able to recall significantly more landmarks at intersections compared to the control group. The number of landmarks at straight segments revealed similar performance for both groups. These results support that the auditory reference to the landmarks at intersections helped to recollect landmark information later. As there was no effect for landmarks at straight segments that received no reference in the instruction, it can be assumed that the processing of the environment was only increased when the landmark-based navigation instructions were provided. Alternative explanations could be that the verbalization of the landmarks increased the concreteness and thus helped to successfully encode information from the environment (Dan Yarmey & Paivio, 1965) or that the combination of visual input and auditory augmentation improved memory encoding (Hsia, 1968). After navigating the route only once, the low quality of the sketch maps did not allow for an analysis of survey knowledge.

The cued-recall task performance was in accordance with the hypothesis that participants using landmark-based navigation instructions acquire more spatial knowledge. There was a significantly increased recognition sensitivity for landmarks at intersections representing incidentally acquired landmark knowledge. This is aligned with previous studies testing

landmark-based navigation instructions during simulated driving in virtual reality (Gramann et al., 2017; Wunderlich & Gramann, 2018). Like in free-recall, the recognition sensitivity for landmarks at straight segments was not enhanced by the landmark-based navigation instructions.

The route knowledge, which was indicated by the route directions when landmarks at intersections were provided as cue, was more accurate when using landmark-based navigation instructions during navigation. Thus, landmark-based instructions enhance the incidental acquisition of route knowledge even after navigating an unfamiliar route only once.

The landmark-based navigation instructions used in the present experiment differed from the standard navigation instructions by naming the landmark as well as by adding more detailed information. Whether the landmark or the level of detail in the instructions enhanced the spatial knowledge acquisition can not be disentangled solely based on the data in the reported experiment. However, in previous experiments, we focused on the impact of different kinds of additional information in landmark-based navigation instructions on spatial knowledge acquisition (Wunderlich & Gramann, 2020). Based on the data from a series of experiments using different landmark-based instructions, it can be stated that landmark-based navigation instructions always enhanced spatial knowledge acquisition compared to standard instructions, whereas the impact of the level of detail in the landmark-based navigation instruction did not consistently add onto this effect. When spatial knowledge was tested directly after assisted navigation more detailed instruction conditions outperformed other conditions whereas when tested several weeks later this additional effect disappeared. Following those results, we can assume that the landmark reference contributed to the differences between navigation instruction conditions.

4.3 | Saccade-related potentials

The analyses of saccade-related potentials revealed clear peaks that were reported previously, including the presaccadic spike potential, the lambda wave, and a clear posterior P2 component. The P100 was most pronounced at POz. This is in line with the lambda response recorded at posterior leads in sERPs and fERPs. Due to the dipolar activity pattern of this component, it is likely that the observed anterior N100 is the negative counterpart of the same source conveyed by volume conduction (Kamienkowski et al., 2012).

sERPs during the straight segments revealed differences between instruction conditions at frontal leads that appeared earlier than the positive component observed with target onset in visual search paradigms (Kamienkowski, Ison, et al., 2012). However, there were no group differences in sERPs during intersections revealing no saccade-related evidence for a visual search triggered by landmark references.

4.4 | Blink-related potentials

More pronounced positive components in the bERP as compared to the sERP point to a difference in information processing after blinks. Blink-related potentials revealed stronger amplitudes at frontal as well as parietal leads with the latter most likely reflecting aspects of visuospatial information processing. Compared to previous studies, the order and polarity of the observed components were roughly comparable to the results reported by Berg and Davies (1988) and Wascher et al. (2014) even though there were differences especially regarding negative components of the potential. The smoother appearance of the presented bERPs compared to Wascher et al. (2014) is likely due to the additional EEG data cleaning and processing steps in the present study.

4.5 | Early blink-evoked components

Opposite polarities of the early ERP peaks at anterior and posterior electrode sites with most pronounced amplitudes over the occipital lobe at the time point of the blink likely reflect volume conducted activity of a radial source in or near the visual cortex. These early peaks evolve parallel with the blink and demonstrate inverse polarity compared to the maximum blink amplitude that served for event-extraction. Since the EOG activity was removed from the EEG data by removing the related independent components, this component is unlikely related to eye or lid movement. It is more likely that the activation of the visual cortex associated with blinks underlies this evoked component. A functional Magnet-Resonance-Tomography study of Tsubota et al. (1999) showed brain activity in the anterior areas of the occipital cortex when blinking in full darkness, which seems to be related to the control of the blink-movement.

Latency differences in the N100 at posterior leads and the P150 at anterior leads speak against the same cortical source underlying these two components. The maximal amplitude and peak width of the N100 at Oz indicate a component originating in the occipital cortex reflecting sensory processing of incoming visual information. In a very simple experiment of Berg and Davies (1988) light sensitivity was already shown in the early peaks of the bERPs at central and posterior electrodes pointing toward a very basic role of these components in visual information processing.

In the present study, the experimental manipulation did not impact the amplitude of these early components. In contrast, the data of Wascher et al. (2014) revealed an early influence of cognitive effort on the P1 component in the

bERP that became more pronounced in the subsequent N2. According to the topography and latency of the N2 as described in Wascher et al. (2014), the comparable component in the present study would be the N250. The absence of a navigation instruction-dependent modulation of these components could then be assumed to reflect comparable mental effort during navigation irrespective of the kind of navigation instruction given.

4.6 | Fronto-central component

At FCz the bERP was sensitive to differences in the navigation instructions during the intersections as reflected in differences from 336 to 772 ms comprising the N300 and the LNC. Compared to the baseline phase, the bERP in the landmark-based navigation instruction condition was increased about 1 μV, while the standard navigation instruction condition remained at the level of the respective baseline bERP. This pattern was visible at several fronto-central leads with increased potentials for the landmark-based navigation instructions. At electrode F2, differences in amplitudes became statistically significant during the N300 and at FC1 during the LNC. This navigation instruction-dependent increase is likely due to fronto-central activity reflecting higher cognitive processes involved in top-down attention allocation in visual search (Li et al., 2010). In the plots of the raw bERP of Wascher et al. (2014) a peak at 400 ms was visible at Fz and Cz only for the cognitive task but not in a rest condition or the physical task. While the authors did not further discuss this pattern, the present data support the assumption of higher cognitive processes underlying the amplitude modulation of the bERP around 300–400 ms. In fixation-related potential studies investigating visual search in complex real-world scenes, a late fronto-central component was revealed in the fERP starting at 300 ms for fixations at a target compared to a distractor face (Kamienkowski et al., 2018; Kaunitz et al., 2014). It seems likely that the landmark-based navigation instructions initiated a visual search for the highlighted landmark. Possibly, this visual search and/or information processing of the additional information was more similar to the cognitive task in the Wascher study, while following standard navigation instructions was rather comparable to their physical task. This fronto-central component was less pronounced in the bERP of the straight segments but remained significant in the LNC at FC1. This general tendency points to a cognitive process (e.g., visual search) that is triggered by landmark-based navigation instructions and takes place especially when instructions are given but remains to some extent active during the entire navigation task, even when walking straight segments of the route. This is in line with the results of the late positive component shown by Wunderlich and Gramann (2018) in the ERPs of the cued-recall task. The significant difference at FC3 seems more likely to be due to the attenuation of a baseline difference between the navigation instruction conditions.

4.7 | Left parietal component

In the bERP of intersections as well as straight segments, a left-lateralized difference in the N250 and P300 components was observed over left centro-parietal and parietal leads (CP5, P7, P5, P3, P1). This modulation was sensitive to the navigation instruction conditions. The landmark-based navigation instruction condition showed lower values in the bERP, while the standard condition remained at a similar level or showed increased values compared to baseline bERPs. The bERP at parietal sites in the study of Wascher et al. (2014) revealed the highest values for rest, followed by the amplitudes in the physical task and most pronounced N2 amplitudes as well as most attenuated P3 amplitudes for the cognitive task. The authors did not discuss lateralized activity but the general parietal focus of the effect is in line with the present results. The direction of the effects would complement the fronto-parietal attention network hypothesis by showing higher amplitudes for standard compared to landmark-based navigation condition persisting in both navigation phases. The observed left-hemispheric dominance at parietal leads was previously shown in the context of motor control and motor planning (Callaert et al., 2011). This could potentially explain why most parietal differences were observed during the baseline phase of the task—right at the start of EEG data collection—and diminish during the following navigation phases.

4.8 | Group differences in baseline

Table 2 and ERPs especially at occipital leads revealed differences between the navigation instruction conditions already during the baseline phase before any navigation instruction was provided to the participants. To understand these baseline differences, we checked demographic and questionnaire data collected alongside with the navigation task. The analysis revealed, that there were some group differences despite the random allocation of participants to the groups. *T* tests comparing the group means pointed to differences for an item relating to the regular use of navigation aids and an item relating to directional knowledge during navigation. The ratings showed that participants of the control group were more confident in their own spatial abilities despite their lower performance in the spatial tasks.

Assuming that the impact of individual spatial abilities on the eye movement-related potentials was constant throughout the assisted navigation task, we decided to control for the baseline differences by subtracting the individual baseline

potential from the respective straight segments- and intersections-potential. This way, the additional impact of the navigation instruction conditions could be revealed despite group differences in the baseline potentials. In case the group difference was only in the baseline phase and not in the following navigation phases, we used the phrase "qualified by baseline difference" in Table 2 to show that the found significant cluster of samples was driven by an effect that diminished with time on task.

However, the absence of a proper baseline is a critical aspect of the present study. The baseline was chosen in a post hoc fashion and was the only time window that was free of any influence from navigation instructions. The baseline phase started with the EEG data collection during preparation and equipping of the participant and its duration varied between participants. Thus, future experiments should include controlled and comparable baseline data collection.

4.9 | Data processing pipeline

Achieving high ecological validity by recording EEG in mobile participants in the real-world increases movement-related artifacts and variability in behavioral and cognitive strategies used to solve the task. As a consequence, the high ecological validity renders the interpretation of the results more difficult (Park et al., 2018). However, the reported data processing pipeline enabled us to successfully extract measures from eye movement-related potentials that were sensitive to changes in visual information processing during free movement in an uncontrolled, real-environment. Remarkably, this was possible based solely on mobile EEG with 64 channels and one EOG electrode. Blink-, saccade-, and gait-related activity could be extracted applying peak detection in the time-domain of respective independent components. Overlapping ERPs were deconvolved and controlled for baseline differences using the unfold toolbox.

An important step was the source-based cleaning that separated the brain from non-brain activity. It is questionable whether the IClabel classification is the best way to do this when investigating mobile EEG as the classifier was trained on stationary, laboratory EEG data. The inclusion of new classification criteria, evaluation, and training based on the data of moving participants would be necessary to refine the classification quality for mobile EEG. Otherwise, IClabel offers a promising approach for automatic source-based data cleaning. We used the default instead of the lite classifier provided by IClabel because it kept a higher number of brain ICs. On average, two additional ICs reached a classification of at least 30% probability to represent a brain source compared to using the lite version of the classifier. We decided to include as many sources as possible for the sensor-based analysis to include all potential brain contributions. In a subjective comparison, the lite classifier seemed to be more conservative and more successful in detecting muscle sources and thus should be favored when aiming for the extraction of source-based measures (see Klug & Gramann, 2020).

Processing the collected mobile EEG data, we realized a strong impact of body movement- and gait-related EEG activity. This impact on the time course of EEG data and the AMICA solution varied between participants. During the automatic event extraction from the time courses of the respective independent components, percentiles were used as values for thresholds that adapt to the individual signal to noise ratio. When applying this event extraction to other tasks those values might have to be adapted. However, especially the 2 Hz artifact elicited by the gait cycle clearly compromised the ERPs. A reduced signal-to-noise ratio of the ERP during walking outdoors compared to sitting inside had been shown when auditory stimuli were presented with a fixed inter-stimulus-interval (Debener et al., 2012). Another study controlling for a possible synchronization of gait and auditory stimulus presentation by adding a jitter reported a comparable signal-to-noise ratio (De Vos et al., 2014). Thus, synchronization of eye movements with the gait-cycle could explain why gait-related EEG activity was especially intrusive to eye movement-related potentials. Even though not assessed in our current study, future studies could investigate individual differences in gait behavior and associated artifacts based on event synchronization with the gait-cycle as well as equipment and analyses approaches emphasizing the importance to control for these factors.

We focused on our processing and results only on ERP measures. Other research has shown that spectral measures related to blinks can add valuable insights (Wascher et al., 2014, 2016).

5 | CONCLUSION

The present study demonstrated that eye movement-related brain potentials can be recorded and analyzed in a meaningful fashion using the real-world as a laboratory. Using blind source separation approaches and subsequent deconvolution of sensor data allowed for extracting brain and non-brain activity that could then be further processed to investigate the impact of navigation instructions on spatial knowledge acquisition. Importantly, using this approach, events representing eye movements like blinks and saccades could be extracted. Those events provide a sufficient number of epochs for event-related potential analyses of the recorded EEG data. This enables new approaches to investigate natural cognition in the real-world.

The results of the blink-related potential analyses confirm that the use of landmark-based navigation instructions leads to variations in the accompanying brain activity. Differences

between auditory navigation instructions are reflected in visual information processing already during the navigation. This difference was mirrored by improved landmark recognition performance of participants that navigated based on landmark instructions.

Future studies will have to replicate the present approach using eye tracking and scene cameras in combination with high-density EEG to establish the link between blinks, saccades, and stimuli-related brain potentials. More importantly, eye tracking in combination with the scene camera will further provide a valuable source to extract additional events from participants' gaze behavior. This will allow for further investigation of the ERP components, comparing eye movement-related ERPs with environment-related events, like fixations on landmarks versus fixations on aspects of the street or other agents like pedestrians or cars.

In conclusion, the present study demonstrates a new analysis approach to investigate human brain activity accompanying complex cognitive tasks in the real-world requiring only mobile EEG recording. This opens up new avenues for a better understanding of the neural foundation of natural cognition.

ACKNOWLEDGMENTS

This research was enabled by a stipend of Stiftung der Deutschen Wirtschaft to A.W. We would like to thank Prof. Matthias Rötting at TU Berlin for providing the car to transport participants, experimenters, and equipment toward and back from the route. Additionally, we give thanks to Maike Fischer, Christopher Hahn as well as Yiru Chen and the students in the neuroergonomics project course for helping to conduct the experiment.

CONFLICTS OF INTEREST

The authors declare that there is no conflict of interest regarding the publication of this paper.

AUTHOR CONTRIBUTIONS

K.G. and A.W. designed the research; A.W. collected the original data; A.W. performed the data analysis and drafted the paper; K.G. and A.W. edited the paper.

PEER REVIEW

The peer review history for this article is available at https://publons.com/publon/10.1111/ejn.15095.

DATA AVAILABILITY STATEMENT

Data relating to these experiments are available upon request from the corresponding author.

ORCID

Anna Wunderlich https://orcid.org/0000-0003-2378-1164
Klaus Gramann https://orcid.org/0000-0003-2673-1832

REFERENCES

Baccino, T. (2012). Eye movements and concurrent event-related potentials: Eye fixation-related potential investigations in reading. In S. P. Liversedge, I. Gilchrist, & S. Everling (Eds), *The Oxford handbook of eye movements* (pp. 857–870). Oxford University Press.

Bell, A. J., & Sejnowski, T. J. (1995). An information-maximization approach to blind separation and blind deconvolution. *Neural Computation*, *7*, 1129–1159.

Bentivoglio, A. R., Bressman, S. B., Cassetta, E., Carretta, D., Tonali, P., & Albanese, A. (1997). Analysis of blink rate patterns in normal subjects. *Movement Disorders*, *12*, 1028–1034.

Berg, P., & Davies, M. B. (1988). Eyeblink-related potentials. *Electroencephalography and Clinical Neurophysiology*, *69*, 1–5.

Bulling A., Ward J. A., Gellersen H., Tröster G. (2011). Eye Movement Analysis for Activity Recognition Using Electrooculography. *IEEE Transactions on Pattern Analysis and Machine Intelligence*, *33*, 741–753. http://dx.doi.org/10.1109/tpami.2010.86

Callaert, D. V., Vercauteren, K., Peeters, R., Tam, F., Graham, S., Swinnen, S. P., Sunaert, S., & Wenderoth, N. (2011). Hemispheric asymmetries of motor versus nonmotor processes during (visuo) motor control. *Human Brain Mapping*, *32*, 1311–1329.

Dahmani, L., & Bohbot, V. D. (2020). Habitual use of GPS negatively impacts spatial memory during self-guided navigation. *Science Reports*, *10*, 1–14.

Dan Yarmey, A., & Paivio, A. (1965). Further evidence on the effects of word abstractness and meaningfulness in paired-associate learning. *Psychonomic Science*, *2*, 307–308.

De Vos, M., Gandras, K., & Debener, S. (2014). Towards a truly mobile auditory brain-computer interface: Exploring the P300 to take away. *International Journal of Psychophysiology*, *91*, 46–53.

Debener, S., Minow, F., Emkes, R., Gandras, K., & de Vos, M. (2012). How about taking a low-cost, small, and wireless EEG for a walk? *Psychophysiology*, *49*, 1617–1621. https://doi.org/10.1111/j.1469-8986.2012.01471.x

Delorme, A., & Makeig, S. (2004). EEGLAB: An open source toolbox for analysis of single-trial EEG dynamics including independent component analysis. *Journal of Neuroscience Methods*, *134*, 9–21.

Dimigen, O., Sommer, W., Hohlfeld, A., Jacobs, A. M., & Kliegl, R. (2011). Coregistration of eye movements and EEG in natural reading: Analyses and review. *Journal of Experimental Psychology General*, *140*, 552–572.

Ehinger, B. V., & Dimigen, O. (2019). Unfold: An integrated toolbox for overlap correction, non-linear modeling, and regression-based EEG analysis. *PeerJ*, *2019*, 1–33. https://doi.org/10.7717/peerj.7838

Evinger, C., Manning, K. A., Pellegrini, J. J., Basso, M. A., Powers, A. S., & Sibony, P. A. (1994). Not looking while leaping: The linkage of blinking and saccadic gaze shifts. *Experimental Brain Research*, *100*, 337–344.

Gaarder, K., Krauskopf, J., Graf, V., Kropfl, W., & Armington, J. C. (1964). Averaged brain activity following saccadic eye movement. *Science*, *146*, 1481–1483.

Gramann, K., Ferris, D. P., Gwin, J., & Makeig, S. (2014). Imaging natural cognition in action. *International Journal of Psychophysiology*, *91*, 22–29.

Gramann, K., Gwin, J. T., Ferris, D. P., Oie, K., Jung, T. P., Lin, C. T., Liao, L. D., & Makeig, S. (2011). Cognition in action: Imaging brain/body dynamics in mobile humans. *Reviews in the Neurosciences*, *22*, 593–608.

Gramann, K., Hoepner, P., & Karrer-Gauss, K. (2017). Navigation instructions for spatial navigation assistance systems lead to incidental spatial learning. *Frontiers in Psychology*, *8*. https://doi.org/10.3389/fpsyg.2017.00193

Hart, S. G. (2006). Nasa-task load index (NASA-TLX); 20 years later. *Proceedings of the Human Factors and Ergonomics Society Annual Meeting*, *50*, 904–908.

Hart, S. G., & Staveland, L. E. (1988). Development of NASA-TLX (Task Load Index): Results of empirical and theoretical research. *Advances in Psychology*, *52*, 139–183.

Hegarty, M., Richardson, A. E., Montello, D. R., Lovelace, K., & Subbiah, I. (2002). Development of a self-report measure of environmental spatial ability. *Intelligence*, *30*, 425–447. https://doi.org/10.1016/S0160-2896(02)00116-2

Hegarty, M., & Waller, D. (2004). A dissociation between mental rotation and perspective-taking spatial abilities. *Intelligence*, *32*, 175–191. https://doi.org/10.1016/j.intell.2003.12.001

Hsia, H. J. (1968). Output, error, equivocation, and recalled information in auditory, visual, and audiovisual information processing with constraint and noise. *The Journal of Communication*, *18*, 325–345.

Ishikawa, T., Fujiwara, H., Imai, O., & Okabe, A. (2008). Wayfinding with a GPS-based mobile navigation system: A comparison with maps and direct experience. *Journal of Environmental Psychology*, *28*, 74–82.

Jacobsen, N. S. J., Blum, S., Witt, K., & Debener, S. (2020). A walk in the park? Characterizing gait-related artifacts in mobile EEG recordings. *European Journal of Neuroscience*, https://doi.org/10.1111/ejn.14965

Jia, Y., & Tyler, C. W. (2019). Measurement of saccadic eye movements by electrooculography for simultaneous EEG recording. *Behavior Research Methods*, *51*, 2139–2151.

Jung, T. P., Makeig, S., Humphries, C., Lee, T. W., Mckeown, M. J., Iragui, V., & Sejnowski, T. J. (2000). Removing electroencephalographic artifacts by blind source separation. *Psychophysiology*, *37*, 163–178. https://doi.org/10.1111/1469-8986.3720163

Kamienkowski, J. E., Ison, M. J., Quiroga, R. Q., & Sigman, M. (2012). Fixation-related potentials in visual search: A combined EEG and eye tracking study. *Journal of Vision*, *12*, 4. https://doi.org/10.1167/12.7.4

Kamienkowski, J. E., Navajas, J., & Sigman, M. (2012). Eye movements blink the attentional blink. *Journal of Experimental Psychology Human Perception Performance*, *38*, 555–560.

Kamienkowski, J. E., Varatharajah, A., Sigman, M., & Ison, M. J. (2018). Parsing a mental program: Fixation-related brain signatures of unitary operations and routines in natural visual search. *NeuroImage*, *183*, 73–86. https://doi.org/10.1016/j.neuroimage.2018.08.010

Kaunitz, L. N., Kamienkowski, J. E., Varatharajah, A., Sigman, M., Quiroga, R. Q., & Ison, M. J. (2014). Looking for a face in the crowd: Fixation-related potentials in an eye-movement visual search task. *NeuroImage*, *89*, 297–305. https://doi.org/10.1016/j.neuroimage.2013.12.006

Kazai, K., & Yagi, A. (2003). Comparison between the lambda response of eye-fixation-related potentials and the P100 component of pattern-reversal visual evoked potentials. *Cognitive, Affective & Behavioral Neuroscience*, *3*, 46–56.

Kline, J. E., Huang, H. J., Snyder, K. L., & Ferris, D. P. (2015). Isolating gait-related movement artifacts in electroencephalography during human walking. *Journal of Neural Engineering*, *12*, 046022. https://doi.org/10.1088/1741-2560/12/4/046022

Klug, M., & Gramann, K. (2020). Identifying key factors for improving ICA-based decomposition of EEG data in mobile and stationary experiments. *The European Journal of Neuroscience*.

Knaepen, K., Mierau, A., Fernandez Tellez, H., Lefeber, D., & Meeusen, R. (2015). Temporal and spatial organization of gait-related electrocortical potentials. *Neuroscience Letters*, *599*, 75–80.

Li, L., Gratton, C., Yao, D., & Knight, R. T. (2010). Role of frontal and parietal cortices in the control of bottom-up and top-down attention in humans. *Brain Research*, *1344*, 173–184.

Lins, O. G., Picton, T. W., Berg, P., & Scherg, M. (1993). Ocular artifacts in EEG and event-related potentials I: Scalp topography. *Brain Topography*, *6*(1), 51–63. https://doi.org/10.1007/BF01234127

Luck, S. J. (2005). An introduction to event-related potentials and their neural origins. In *An Introduction to the Event-Related Potential Technique*, 1st edn., Tech., MIT Press.

Luck, S. J., Heinze, H. J., Mangun, G. R., & Hillyard, S. A. (1990). Visual event-related potentials index focused attention within bilateral stimulus arrays. II. Functional dissociation of P1 and N1 components. *Electroencephalography and Clinical Neurophysiology*, *75*, 528–542.

Luck, S. J., Woodman, G. F., & Vogel, E. K. (2000). Event-related potential studies of attention. *Trends Cognitive in Sciences*, *4*, 432–440.

Makeig, S., Bell, J. A., Jung, T.-P., & Sejnowski, T. J. (1996). Independent component analysis of electroencephalographic data. *Advances in Neural Information Processing Systems*, *8*, 145–151.

Makeig, S., Gramann, K., Jung, T. P., Sejnowski, T. J., & Poizner, H. (2009). Linking brain, mind and behavior. *International Journal of Psychophysiology*, *73*, 95–100.

Marton, M., & Szirtes, J. (1988). Context effects on saccade-related brain potentials to words during reading. *Neuropsychologia*, *26*, 453–463. https://doi.org/10.1016/0028-3932(88)90098-X

Münzer, S., Fehringer, B. C. O. F., & Kühl, T. (2016). Validation of a 3-factor structure of spatial strategies and relations to possession and usage of navigational aids. *Journal of Environmental Psychology*, *47*, 66–78.

Münzer, S., & Hölscher, C. (2011). Entwicklung und validierung eines fragebogens zu räumlichen strategien. *Diagnostica*, *57*, 111–125. https://doi.org/10.1026/0012-1924/a000040

Münzer, S., Zimmer, H. D., Schwalm, M., & Baus, J. (2006). Computer assisted navigation and the aquisition of route and survey knowledge. *Journal of Environmental Psychology*, *26*, 300–308.

Oliveira, A. S., Schlink, B. R., Hairston, W. D., König, P., & Ferris, D. P. (2017). A Channel rejection method for attenuating motion-related artifacts in EEG recordings during walking. *Frontiers in Neuroscience*, *11*, 1–17.

Oostenveld, R., & Oostendorp, T. F. (2002). Validating the boundary element method for forward and inverse EEG computations in the presence of a hole in the skull. *Human Brain Mapping*, *17*, 179–192.

Oostenveld, R., & Praamstra, P. (2001). The five percent electrode system for high-resolution EEG and ERP measurements. *Clinical Neurophysiology*, *112*, 713–719.

Ossandón, J. P., Helo, A. V., Montefusco-Siegmund, R., & Maldonado, P. E. (2010). Superposition model predicts EEG occipital activity during free viewing of natural scenes. *The Journal of Neuroscience*, *30*, 4787–4795.

Palmer, J., Kreutz-Delgado, K., & Makeig, S. (2011). *AMICA: An adaptive mixture of independent component analyzers with shared components*. Tech. report, Swart. Cent. Comput., Neurosci., San Diego, CA, 1–15.

Park, J. L., Dudchenko, P. A., & Donaldson, D. I. (2018). Navigation in real-world environments: New opportunities afforded by advances in mobile brain imaging. *Frontiers in Human Neuroscience*, *12*. https://doi.org/10.3389/fnhum.2018.00361

Pion-Tonachini, L., Kreutz-Delgado, K., & Makeig, S. (2019). ICLabel: An automated electroencephalographic independent component classifier, dataset, and website. *NeuroImage*, *198*, 181–197. https://doi.org/10.1016/j.neuroimage.2019.05.026

Rämä, P., & Baccino, T. (2010). Eye fixation-related potentials (EFRPs) during object identification. *Visual Neuroscience*, *27*, 187–192.

Sailer, U., Güldenpfennig, F., & Eggert, T. (2016). Saccade-related potentials during eye-hand coordination: Effects of hand movements on saccade preparation. *Motor Control*, *20*, 316–336. https://doi.org/10.1123/mc.2015-0018

Simola, J., Holmqvist, K., & Lindgren, M. (2009). Right visual field advantage in parafoveal processing: Evidence from eye-fixation-related potentials. *Brain and Language*, *111*, 101–113. https://doi.org/10.1016/j.bandl.2009.08.004

Snyder, K. L., Kline, J. E., Huang, H. J., & Ferris, D. P. (2015). Independent component analysis of gait-related movement artifact recorded using EEG electrodes during treadmill walking. *Frontiers in Human Neuroscience*, *9*, 1–13.

Stern, J. A., Walrath, L. C., & Goldstein, R. (1984). The endogenous eyeblink. *Psychophysiology*, *21*, 22–33. https://doi.org/10.1111/j.1469-8986.1984.tb02312.x

Tsubota, K., Kwong, K. K., Lee, T.-Y., Nakamura, J., & Cheng, H.-M. (1999). Functional MRI of brain activation by eye blinking. *Experimental Eye Research*, *69*, 1–7.

Wascher, E., Heppner, H., & Hoffmann, S. (2014). Towards the measurement of event-related EEG activity in real-life working environments. *International Journal of Psychophysiology*, *91*, 3–9.

Wascher, E., Heppner, H., Kobald, S. O., Arnau, S., Getzmann, S., & Möckel, T. (2016). Age-sensitive effects of enduring work with alternating cognitive and physical load. A study applying mobile EEG in a real life working scenario. *Frontiers in Human Neuroscience*, *9*, 1–14. https://doi.org/10.3389/fnhum.2015.00711

Wunderlich, A., & Gramann K. (2018). Electrocortical Evidence for Long-Term Incidental Spatial Learning Through Modified Navigation Instructions. In: S. Creem-Regehr, J. Schöning, & A. Klippel (Eds), *Spatial Cognition XI. Spatial Cognition 2018. Lecture Notes in Computer Science*, vol 11034. Springer, Cham. https://doi.org/10.1007/978-3-319-96385-3_18

Wunderlich, A., & Gramann, K. (2020). Landmark-based navigation instructions improve incidental spatial learning in real-life environments. *bioRXiv*, 1–36.

How to cite this article: Wunderlich A, Gramann K. Eye movement-related brain potentials during assisted navigation in real-world environments. *Eur J Neurosci*. 2021;00:1–19. https://doi.org/10.1111/ejn.15095